A genetic link between leaf carbon isotope composition and whole-plant water use efficiency in the C_4 grass *Setaria*

Patrick Z. Ellsworth (0000-0002-0795-5200)[1], Max J. Feldman (0000-0002-5415-4326)[2], Ivan Baxter (0000-0001-6680-1722)[2,] Asaph B. Cousins (0000-0003-2424-714X)[1]
[1]School of Biological Sciences, Washington State University
[2]Donald Danforth Plant Sciences Center

Summary

- Genetic selection for whole plant water use efficiency (yield per transpiration; WUE_{plant}) in any crop-breeding program requires high throughput phenotyping of component traits of WUE_{plant} such as transpiration efficiency (TE_i; CO_2 assimilation rate per stomatal conductance). Leaf carbon stable isotope composition ($\delta^{13}C_{leaf}$) has been suggested as a potential proxy for WUE_{plant} because both parameters are influenced by TE_i. However, a genetic link between $\delta^{13}C_{leaf}$ and WUE_{plant} in a C_4 species is still not well understood.
- Therefore, a high throughput phenotyping facility was used to measure WUE_{plant} in a recombinant inbred line (RIL) population of the C_4 grasses *Setaria viridis* and *S. italica* to determine the genetic relationship between $\delta^{13}C_{leaf}$, WUE_{plant}, and TE_i under well-watered and water-limited growth conditions.
- Three quantitative trait loci (QTL) for $\delta^{13}C_{leaf}$ were found to co-localize with transpiration, biomass accumulation, and WUE_{plant}. WUE_{plant} calculated for each of the three $\delta^{13}C_{leaf}$ allele classes was negatively correlated with $\delta^{13}C_{leaf}$ as would be predicted when TE_i is driving WUE_{plant}.
- These results demonstrate that $\delta^{13}C_{leaf}$ is genetically linked to WUE_{plant} through TE_i and can be used as a high throughput proxy to screen for WUE_{plant} in these C_4 species.

Key words: quantitative trait loci, leaf carbon isotopes, C_4 photosynthesis, *Setaria*, water use efficiency, phenotyping, genetic architecture, drought, transpiration efficiency

Introduction

Water availability constrains agricultural production and threatens food security in many drought-prone regions (Morison *et al.*, 2008). Therefore, improving the harvestable yield relative to water supplied to crop systems (agronomic water use efficiency; WUE_{ag}) has long received attention from researchers and government agencies (Bierhuizen & Slatyer, 1965; Passioura, 1977; Sinclair *et al.*, 1984; Vadez *et al.*, 2014). It has been proposed by Passioura (1977) that yield could be improved relative to available water by increasing (1) the ratio of transpiration (T) to evapotranspiration (ET), (2) whole plant water use efficiency (ratio of biomass production to total transpiration; WUE_{plant}), and (3) harvest index (HI). To date, increases in WUE_{ag} have been primarily made by improved management practices that increase T/ET such as reducing runoff and evaporation from the soil through improved irrigation methods (Deng *et al.*, 2006; Medrano *et al.*, 2015a), increased canopy cover (Westgate *et al.*, 1997) and mulching (Medrano *et al.*, 2015a). Additionally, selecting for greater HI has increased WUE_{ag}, for example, with semi-dwarf wheat varieties (Richards *et al.*, 2014). As improvements in WUE_{ag} through management practice reach their theoretical maximum, the greatest increases in WUE_{ag} will be through improved WUE_{plant}, which have so far been minimal (Condon *et al.*, 2004; Deng *et al.*, 2006; Medrano *et al.*, 2015a).

To date, the limited improvement in WUE_{plant} is primarily because WUE_{plant} is a complex trait that is influenced by 1) net CO_2 assimilation (A_{net}) relative to water loss via stomatal conductance (g_s), (i.e. the intrinsic transpiration efficiency, A_{net}/g_s; TE_i), 2) the proportion of carbon loss from whole plant respiration (ϕ_c), 3) "unproductive" water loss from cuticular and nighttime transpiration (ϕ_w), and 4) the evaporative demand between the atmosphere and the plant (See theory section; Farquhar & Richards, 1984; Farquhar, Graham D. *et al.*, 1989; Farquhar, G. D. *et al.*, 1989). Theoretically, the first three of these factors can be selected for through plant breeding, but these traits, especially ϕ_c and ϕ_w, are determined by a complex set of traits that are difficult to measure and select for in breeding programs (Condon *et al.*, 2002; Flexas *et al.*, 2010; Coupel-Ledru *et al.*, 2016). Alternatively, in theory, TE_i is an ideal trait to select for because it is independent of environmental conditions driving changes in evaporative demands (Ghannoum, 2016), and it is an important component of WUE_{plant} because it relates to both CO_2 and H_2O leaf exchange, influencing both photosynthetic capacity and T (Condon *et al.*, 2002; Condon *et al.*, 2004). Unfortunately, the primary method of estimating TE_i is by gas exchange measurements of A_{net}/g_s that do not integrate well

over time and generally do not represent TE_i over the lifetime of the plant or even the leaf (Condon *et al.*, 2004). Furthermore, these measurements are prohibitively time-consuming and laborious, making this method impractical for selecting for WUE_{plant} in a plant-breeding program; thus, a high throughput proxy of WUE_{plant} is needed.

Alternatively, leaf carbon isotope composition ($\delta^{13}C_{leaf}$) has long been promoted as a proxy for an integrated measurement of TE_i in C_3 and potentially in C_4 species (Farquhar, 1983; Farquhar & Richards, 1984; Condon *et al.*, 1987; Farquhar, Graham D. *et al.*, 1989; Farquhar, G. D. *et al.*, 1989). In C_3 plants, the relationship between $\delta^{13}C_{leaf}$ and TE_i has been tested and even integrated into breeding programs (Farquhar & Richards, 1984; Condon *et al.*, 2002; Condon *et al.*, 2004; Cabrera-Bosquet, L. *et al.*, 2009; Cabrera-Bosquet *et al.*, 2011; Cabrera-Bosquet *et al.*, 2012; Elazab *et al.*, 2012; Yousfi *et al.*, 2012; Araus *et al.*, 2013). However, it remains uncertain if $\delta^{13}C_{leaf}$ is an effective proxy of TE_i in C_4 species because it has not been determined if there is adequate response in $\delta^{13}C_{leaf}$ to TE_i and if there is genotypic variation in $\delta^{13}C_{leaf}$ that has a physiological relationship with WUE_{plant}. Nonetheless, empirical evidence in multiple C_4 species such as *Setaria viridis*, *S. italica*, *Zea mays*, and *Sorghum bicolor* supports the theoretical relationship between $\delta^{13}C_{leaf}$ and TE_i (Henderson *et al.*, 1998; Cabrera-Bosquet *et al.*, 2009; Ellsworth *et al.*, 2017). These studies also demonstrated consistent differences in $\delta^{13}C_{leaf}$ between well-watered and water-limited plants that negatively correlated with TE_i. Additionally, in *S. viridis* and *S. italica*, TE_i correlated with WUE_{plant} (Ellsworth *et al.*, 2017). However, a correlation between TE_i and WUE_{plant} has not always been found in C_3 and C_4 species (Terashima & Hikosaka, 1995; Gibberd *et al.*, 2001; Cerasoli *et al.*, 2004; Xu & Hsiao, 2004; Chaves *et al.*, 2007; Poni *et al.*, 2009; Tarara *et al.*, 2011; Tomás *et al.*, 2012; Tomás *et al.*, 2014; Medrano *et al.*, 2015b; Pinto *et al.*, 2015). Therefore, further investigations are needed to delineate the component traits, including TE_i, that collectively compose WUE_{plant} and how they affect the relative importance of TE_i to WUE_{plant}, particularly in C_4 plants.

The genetic control of WUE_{plant} and its relationship to TE_i and $\delta^{13}C_{leaf}$ can potentially be identified using large mapping populations grown on automated phenotyping systems that measure whole plant water use and biomass accumulation on hundreds of individual plants (Fahlgren *et al.*, 2015; Feldman *et al.*, 2018). Therefore, the physiological traits, biomass accumulation, transpiration, WUE_{plant}, and $\delta^{13}C_{leaf}$, can be studied to determine their genetic architecture and relationships. In fact, quantitative

trait loci (QTL) have been found for $\delta^{13}C_{leaf}$ in several C_3 species such as rice (Takai *et al.*, 2006; Takai *et al.*, 2009; Xu *et al.*, 2009), barley (Teulat *et al.*, 2002), *Brachypodium distachyon* (Des Marais *et al.*, 2016), wheat (Rebetzke *et al.*, 2008), tomato (Xu *et al.*, 2008), *Arabidopsis* (Juenger *et al.*, 2005; McKay *et al.*, 2008), sunflower (Adiredjo *et al.*, 2014), soybean (Dhanapal *et al.*, 2015), cotton (Saranga *et al.*, 2004), *Quercus robur* (Brendel *et al.*, 2008), and *Stylosanthes scabra* (Thumma *et al.*, 2001). Additionally, a few studies on C_3 plants have found co-localized QTL for $\delta^{13}C_{leaf}$ and WUE_{plant} (Adiredjo *et al.*, 2014; Easlon *et al.*, 2014), and, in one case, $\delta^{13}C_{leaf}$ and TE_i were associated with a causal gene (ERECTA; Masle *et al.*, 2005). However, to date only in two studies $\delta^{13}C$ was found to be under genetic control in a C_4 species (maize; Gresset *et al.*, 2014; Twohey III *et al.*, 2018), and in a follow-up study a genomic region was identified that affected both $\delta^{13}C_{leaf}$ and WUE_{plant} (Avramova *et al.*, 2018). Now more research is necessary to develop a more thorough understanding of the physiological relationship and genetic architecture of $\delta^{13}C_{leaf}$, TE_i, and WUE_{plant}, so that marker-assisted breeding can be effectively used to select for WUE_{plant} and TE_i in C_4 plants.

Here a recombinant inbred line (RIL) population of 189 lines created from accession A10 of *S. viridis* (L.) P. Beauv. and accession B100 of *S. italica* (L.) P. Beauv. was used to screen for WUE_{plant}, TE_i, and $\delta^{13}C_{leaf}$ (Devos *et al.*, 1998; Wang *et al.*, 1998; Feldman *et al.*, 2018). Both *S. viridis* and *S. italica* are model C_4 grasses in the same panicoid clade as important C_4 crops such as maize, sugarcane, sorghum, Miscanthus, and the emerging bioenergy crop switchgrass. The objectives of this study were to compare $\delta^{13}C_{leaf}$ between plants grown under well-watered and water-limited conditions and to determine the genetic and physiological relationship between WUE_{plant}, TE_i, and $\delta^{13}C_{leaf}$.

Theory

Agricultural water use efficiency (WUE_{ag}) can be defined as the crop yield per unit water supplied to the crop system. Where crop yield relative to water use can be calculated as a function of evapotranspiration (ET), the proportion of ET that is transpired (T/ET), WUE_{plant}, and the harvest index (harvested proportion of biomass; Eqn 1; Passioura, 1977; Condon *et al.*, 2002) as

$$Yield = ET\ x\ \frac{T}{ET}\ x\ WUE_{plant}\ x\ HI. \qquad \text{Equation 1}$$

133 WUE_{ag} can be improved by maximizing the proportion of water inputs that are
134 transpired at the field scale, increasing the ratio of biomass produced to water
135 transpired, and improving the harvestable portion of the crop. Increasing the
136 proportion of water transpired can be obtained through better crop and water
137 management. On the other hand, the ratio of biomass and water transpired is a
138 physiological process incapsulated in WUE_{plant} and improving WUE_{plant} is an important
139 factor in increasing WUE_{ag} because it relates the fundamental relationship between
140 carbon and water flux between the plant and its environment.

141 WUE_{plant} relates to net CO_2 assimilation rates (A_{net}) relative to transpiration rate
142 (T) at the whole plant level, and accounts for the proportion of fixed carbon that is lost
143 (ϕ_c) such as respiration and the proportion of water loss that is "unproductive" (ϕ_w)
144 such as nighttime transpiration (T_{night}) or cuticular evaporation because it is not
145 associated with CO_2 assimilation (Eqn 2; Farquhar, Graham D. *et al.*, 1989; Seibt *et al.*,
146 2008). The relationship of these parameters to WUE_{plant} can be defined as

$$WUE_{plant} = \frac{A_{\text{net}}(1-\phi_c)}{T(1+\phi_w)} \qquad \text{Equation 2}$$

147 where A_{net} and T are related through stomatal conductance (g_s) as

$$A_{\text{net}} = g_{sCO2}(C_a - C_i) \qquad \text{Equation 3}$$

148 and

$$T = g_{sH2O}(e_i - e_a). \qquad \text{Equation 4}$$

149 The parameter (e_i - e_a) is the water vapor molar difference between intercellular and
150 ambient air at leaf temperature, (C_a - C_i) is the CO_2 molar difference between
151 intercellular and ambient CO_2, and g_{sCO2} and g_{sH2O} are the conductance values for CO_2
152 and H_2O, respectively (Farquhar & Richards, 1984; Farquhar, Graham D. *et al.*, 1989;
153 Farquhar, G. D. *et al.*, 1989). Substituting Eqns 3 and 4 into Eqn 2 gives

$$WUE_{plant} = \frac{g_{sCO2}(C_a - C_i)(1-\phi_c)}{g_{sH2O}(e_i - e_a)(1+\phi_w)} = \frac{C_a\left(1-\frac{C_i}{C_a}\right)(1-\phi_c)}{1.6v(1+\phi_w)} \quad \text{Equation 5}$$

where v is the evaporative demand (e_i-e_a), and the ratio of diffusivities of H_2O and CO_2 in air is 1.6. The molar ratio of intercellular to ambient CO_2 (C_i/C_a) influences WUE_{plant} because it represents the relative drawdown of intercellular CO_2 (C_i) by photosynthesis and the conductance of CO_2 into the leaf and the conductance of water vapor out the leaf via the stomata. Intrinsic TE (A_{net}/g_s; TE_i) is equal to the CO_2 gradient from ambient to intercellular spaces (C_i - C_a), which can be rewritten as $C_a(1\text{-}C_i/C_a)$. Therefore, Eqn 5 can be simplified as a function of TE_i (Eqn 6). TE_i and leaf carbon composition ($\delta^{13}C_{leaf}$) form a relationship through their common relationship with C_i/C_a.

$$WUE_{plant} = \frac{TE_i(1-\phi_c)}{1.6v(1+\phi_w)} \quad \text{Equation 6}$$

The relationship between $\delta^{13}C_{leaf}$ and TE_i is based on 1) variation in $\delta^{13}C_{leaf}$ (‰) of plants grown in the same atmospheric conditions is primarily controlled by leaf CO_2 isotope discrimination ($\Delta^{13}C$), 2) $\Delta^{13}C$ is influenced by changes in C_i/C_a and 3) C_i/C_a, as stated above, is affected by the interrelationship A_{net} and g_s. Therefore, TE_i (A_{net}/g_s) is related to C_i/C_a and, in turn, $\Delta^{13}C$ (Farquhar, G. D. *et al.*, 1989; Henderson *et al.*, 1998).

Finally, $\Delta^{13}C_{leaf}$ is related to $\delta^{13}C$ as

$$\Delta^{13}C = \frac{\delta^{13}C_{ambient} - \delta^{13}C_{leaf}}{1+\delta^{13}C_{leaf}} \quad \text{Equation 7}$$

where, $\delta^{13}C_{leaf}$ and $\delta^{13}C_{ambient}$ are the $^{13}C/^{12}C$ ratios of the leaf and the CO_2 in the air surrounding the leaf, respectively (Farquhar, 1983). In C_4 species, $\Delta^{13}C$ is primarily determined by fractionations associated with CO_2 carboxylation and diffusion, the ratio of bundle sheath CO_2 leak rate to PEP carboxylase rate (leakiness; ϕ), and C_i/C_a (Eqn 8). Leakiness (ϕ) determines the slope of the relationship between $\Delta^{13}C$ and C_i/C_a. Based on this mathematical relationship, if ϕ is less than 0.37, then $\Delta^{13}C$ increases as C_i/C_a decreases, which corresponds with increasing $\delta^{13}C_{leaf}$. If ϕ is greater than 0.37, then the relationship reverses where $\Delta^{13}C$ increases with C_i/C_a. In *Setaria*, ϕ has been found to be

less than 0.37, so C_i/C_a is expected to form a negative relationship with $\Delta^{13}C$ and positive relationship with $\delta^{13}C_{leaf}$ (Ellsworth et al. unpublished; Kubásek *et al.*, 2007). Variation in ϕ across genotypes could reduce or eliminate the relationship between $\delta^{13}C_{leaf}$ and TE_i (and WUE_{plant}). This is because differences in ϕ between plants with the same C_i/C_a (and same TE_i) would differ in carbon discrimination and $\delta^{13}C_{leaf}$, while other individuals that differ in C_i/C_a and ϕ would have the same $\delta^{13}C_{leaf}$, confounding the relationship between $\delta^{13}C_{leaf}$ and TE_i. However, ϕ has been shown to be relatively constant across many C_4 species and across environmental conditions such as light intensities, salinity, and CO_2 partial pressures (Ubierna *et al.*, 2011; Sun *et al.*, 2012; Bellasio, C. & Griffiths, H., 2014; Kromdijk *et al.*, 2014; Sage, 2014; Sharwood *et al.*, 2014; Sonawane *et al.*, 2017; Sonawane *et al.*, 2018).

The relationship of $\Delta^{13}C$ and C_i/C_a can be defined by simplifying the relationship that was originally described by Farquhar (1984) as

$$\Delta^{13}C = a + (b_4 + \phi(b_3 - s) - a)\frac{C_i}{C_a} \qquad \text{Equation 8}$$

where a is the fractionation during diffusion of CO_2 in air through stomata (4.4 ‰), b_4 is the fractionations of PEP carboxylation and the preceding isotopic equilibrium during dissolution and hydration of CO_2 (-5.7 ‰ at a leaf temperature of 25 °C) as described in (Mook *et al.*, 1974; Henderson *et al.*, 1992), b_3 is the Rubisco fractionation (29 ‰), and s is the fractionation during the leakage of CO_2 out of the bundle sheath cells (1.8 ‰) (Henderson *et al.*, 1992; Henderson *et al.*, 1998). The CO_2 concentrating mechanism in C_4 species reduces Rubisco isotopic discrimination against ^{13}C, so that the response of $\Delta^{13}C$ (and $\delta^{13}C_{leaf}$) across a gradient of C_i/C_a is dampened relative to that in C_3 species (von Caemmerer *et al.*, 2014). As a result, variation in $\delta^{13}C_{leaf}$ with respect to TE_i is related to their mutual relationship with C_i/C_a.

Methods

Plant material and growth conditions

An interspecific *Setaria* F7 recombinant inbred line (RIL) population comprised of 189 genotypes was previously generated through a cross between the wild-type green foxtail *S. viridis* accession, A10, and the domesticated *S. italica* foxtail millet accession, B100 (Devos *et al.*, 1998; Wang *et al.*, 1998; Doust *et al.*, 2009). Seeds from this population were sowed in 10 cm diameter pots pre-filled with ~470 cm^3 of Metro-Mix 360 soil (Hummert, USA) and 0.5 g of Osmocote Classic 14-14-14 fertilizer (Everris, USA) and

placed on the Bellwether Phenotyping System using an alpha lattice design replicating each genotype and treatment combination three times. Two to three replicates per genotype, including the A10 and B10 parental accessions, per treatment (1138 individuals) were transferred to the Bellwether Phenotyping System at 8 days after sowing. The experiment continued for 25 days with a photoperiod of 16 h light / 8 h night, light intensity of 500 μmol/m²/s, a temperature regime of 31 °C day/21 °C night and relative humidity was maintained between 40 – 80 % (Feldman *et al.*, 2018). For each replicate of each genotype, one individual plant from the well-watered treatment was grown next to a plant in the water-limited treatment. The position in the growth chamber of each paired replicates was randomly assigned and did not change during the experiment. The effect of growth chamber location was found to be negligible.

Plants were divided into two treatments: well-watered and water-limited, where soil water content was maintained at 100 % or 40 % of pot capacity (PC), respectively. Initially all seedlings were watered to pot capacity for the first two days at the Bellwether Foundation Phenotyping Facility at the Danforth Center (Feldman *et al.*, 2017; Feldman *et al.*, 2018). After two days, the potting medium in the water-limited treatment was not watered until water content dropped to 40 % PC, at which point watering resumed. To maintain soil water content at prescribed treatment levels (well-watered 100 % PC; water-limited 40 % PC), plants were watered 2 times per day until day 26 when the plants began to be watered three times per day. At this point watering took place when the light turned on, midday, and when the lights turned off. Pots were watered by weighing them and adding water until the pot weight returned to a preset weight calculated as either 100 or 40 % PC in the well-watered and water-limited treatments, respectively, as determined by Fahlgren *et al.* (2015). Prescribed soil water content across both treatment blocks was achieved by 15 days after planting. Additional detail on the experimental design and plant growth can be found in Feldman *et al.* (2017); Feldman *et al.* (2018).

Measurements of biomass and transpiration

RGB images of individual plants were acquired using a side view camera at four different angular rotations (0°, 90° 180°, 270°) every other day, which was used to calculate biomass dry weight (Fahlgren *et al.*, 2015; Feldman *et al.*, 2018). Optical zoom was adjusted during the experiment to ensure optimal images for plant size measurements. Scaling factors relating pixel area to ground truth measurements were

used to translate pixels to relative area (pixels/cm^2). The sensitivity of the measurements limited reliable measurements of plant size and transpiration to a period from day 17 to 33 when plants were sufficiently large for accurate image analysis and measurements of transpiration (Feldman *et al.*, 2018). After the experiment concluded, 176 individual plants (91 plants from the 100 % FC and 85 from the 40 % FC) were randomly harvested and weighed for fresh aboveground biomass. Dry aboveground biomass was measured after drying at 60 °C for three days. The linear relationship between plant area from a side-view and dry aboveground biomass produced a goodness of fit similar to more complex models with multiple explanatory variables such as top-view plant area and plant height but did not overfit the data ($R^2 = 0.74$). A loess function (default parameters) was used to smooth the data in the R stats library to interpolate aboveground dry biomass on an individual genotype within treatment (Chambers & Hastie, 1992). To avoid error propagation, all analyses were conducted on side-view plant area (in pixels), and after the analyses, side-view plant area was converted to dry aboveground biomass (Feldman *et al.*, 2018).

The LemnaTec instrument at the Bellwether Phenotypying Facility provided the volume of water transpired by individual plants based on gravimetric measurements and from which water use efficiency (WUE_{plant}) was calculated. Total daily transpired water was the difference in total water added to the pot minus the total water added to empty pots on each calendar day. Empty pots were maintained in both the well-watered and water-limited treatments. Total water added was calculated as the difference between the measured pot weight and the weight of the pre-filled pot or the difference between current pot weight and the weight measurement on the previous day if no water was added. Empty pots were included in the experimental design to determine the volume of water lost through soil evaporation and to separate it from transpired water. Therefore, the cumulative transpiration on day 27 was the sum of all water transpired from day 17 until day 27. As described in (Feldman *et al.*, 2018), day 17 was when the difference transpired water and soil evaporation was sufficiently large to accurately measure the volume of transpired water. On days 27-33, we were able to divide plant transpiration into daytime and nighttime components because the irrigation schedule increased from two to three daily waterings, including when the lights turned on in the morning and off at night. WUE_{plant} was calculated as the ratio of dry aboveground biomass to total water transpired.

Leaf carbon stable isotopic composition ($\delta^{13}C_{leaf}$)

As a point of reference, results for genotypic and treatment effect on traits was conductance on day 27 instead of using all days and compared to $\delta^{13}C_{leaf}$. The plants on day 27 were in vegetative phase and growing rapidly, typical of when physiological and gas exchange measurements would be made. Additionally, day 27 was representative in terms of QTL and other analyses conducted throughout the experiment (Feldman *et al.*, 2018). To not interrupt the experiment, the $\delta^{13}C_{leaf}$ had to be collected from a harvested leaf at the end of the experiment (day 34). The leaf collected for $\delta^{13}C_{leaf}$ was the youngest, uppermost, fully expanded leaf, which is the same age and development as a leaf that would have been collected on day 27 if that had been possible.

The leaves were dried at 60 °C for three days, and then 8-12 discs, having a total leaf area of 0.47 – 0.71 cm^2, were sampled from each leaf and placed in tin capsules for stable isotopic analysis. A comparison of $\delta^{13}C_{leaf}$ from sampling leaf discs versus sampling an aliquot of the completely homogenized powered leaf tissue was made on a subset of 47 leaves. The slope of $\delta^{13}C_{leaf}$ from the punches regressed against $\delta^{13}C_{leaf}$ from the ground leaf tissue was 0.93 ± 0.03 (R^2 = 0.96; Fig. **S1**), and the mean difference between methods was 0.06 ± 0.04 ‰, which was similar to the IRMS precision for carbon stable isotope analysis and substantially less than the sample standard deviation of 0.5 ‰. Considering the similarity between sampling methods, all leaves were sampled using the more rapid leaf disc method.

Leaf tissue was converted to CO_2 with an elemental analyzer (ECS 4010, Costech Analytical, Valencia, CA) and analyzed with a continuous flow isotope ratio mass spectrometer (Delta PlusXP, ThermoFinnigan, Bremen; Brenna *et al.*, 1997; Qi *et al.*, 2003). The Santrock correction was used by the IRMS software to correct for ^{17}O (Santrock *et al.*, 1985). Final δ values were the mean of 5 sample peaks calibrated to the international standards NBS 19, RM 8542, and IAEA-CO-9 to calculate $\delta^{13}C$ relative to Vienna Peedee belemite (V-PDB). Quality control standards were also included to determine the correction quality. Overall standard deviation for $\delta^{13}C$ values was 0.07 ‰.

The stable isotope composition of carbon ($\delta^{13}C_{leaf}$) was reported in δ notation,

$$\delta = \left(\frac{R_{sample}}{R_{standard}} - 1\right) \quad \text{Equation 9}$$

where R_{sample} and $R_{standard}$ is the isotopic ratios of carbon ($^{13}C/^{12}C$) of the sample and international standard, respectively. The international standard used for oxygen was Vienna- PeeDee Belemite (VPDB).

QTL analysis

The same methods used in Feldman *et al.* (2017); Feldman *et al.* (2018) were used in this study, and here the methods used are repeated. QTL mapping was performed on day 27 within each treatment group using functions in the R/qtl and funqtl packages (Kwak *et al.*, 2016). The functions were called by a set of custom Python and R scripts (https://github.com/maxjfeldman/foxy_qtl_pipeline). Two complimentary analysis methods were utilized. First, a single QTL model genome scan using Haley-Knott regression was performed to identify QTL exhibiting LOD score peaks greater than a permutation-based significance threshold ($\alpha = 0.05$, n = 1000). Second, a stepwise forward/backward selection procedure was used to identify an additive, multiple QTL model based upon maximization of penalized LOD score.

The function-valued approach described by Kwak *et al.* (2016) was used to identify QTL associated with the average (SLOD) and maximum (MLOD) score at each locus throughout the experiment. Each genotypic mean trait within treatments was estimated using loess smoothing, and the QTL significance threshold was determined based upon the permutation-based likelihood of observing the empirical SLOD or MLOD test statistic. Separate, independent linkage mapping analysis performed at each time point identified a larger number of QTL locations relative to similar function-valued analysis based on the SLOD and MLOD statistics calculated at each marker. After refinement of QTL position estimates, the significance of fit for the full multiple QTL model was assessed using type III ANOVA. The contribution of individual loci was assessed using drop-one-term, type III ANOVA. The absolute and relative allelic effect sizes were determined by comparing the fit of the full model to a sub-model with one of the terms removed. QTL were grouped by finding the largest QTL by proportional variance explained and combining all QTL within 10 cM of it, then this was done for the next largest QTL and so on until all QTL were accounted for. All putative protein-coding genes (*Setaria viridis* genome version 1.1)

found within a 1.5-logarithm of the odds (LOD) confidence interval were reported for each QTL in Feldman et al. (2018), which includes all QTL found in this study as well. Epistasis between QTL was evaluated using the same method as in Feldman *et al.* (2018) and Feldman *et al.* (2017) by comparing the log10 likelihood ratio of a model describing the additive effect and the additive interaction between two QTL with a model only containing the additive interaction between the two QTL. The significance threshold was determined through permutation (α = 0.05, n = 100).

Statistical analysis

Statistical analyses were conducted in R version 3.4.0 (R Team R_Core_Team, 2013). Homogeneity was tested based on plotting predicted fit versus residuals. Using the extRemes package (version 2.0-8), normality was tested by plotting residuals on quantiles-quantiles plots. Within treatment comparisons were made on each trait using a two-factor analysis of variance (ANOVA) where the factors were treatment and genotype. Broad-sense heritability was calculated the proportion of total variance of a trait is attributed to genotypic variation ($H^2 = \sigma^2_{genotypic}/\sigma^2_{total}$). Using lmodel2 (version 1.7-2) package, model II regression analysis (standard major axis) were used instead of ordinary least squares regression for all linear regressions because neither variable was controlled, both varied naturally with their own associated error, and the physical units of both variables were not the same. Two-way ANOVAs were used to determine if the effect of treatment and genotype on each trait was significant.

Results

Dry biomass, transpiration, and WUE_{plant} *traits*

Whole plant biomass accumulation and total transpiration were analyzed throughout the experiment, and their relationship remained relatively constant through time (Fig. **S1**; Feldman *et al.*, 2018). We selected day 27 for our analysis when all genotypes were in the vegetative stage. On this day, dry biomass estimated from side view images and validated with final harvest biomass (Feldman *et al.*, 2018) varied significantly across genotypes from 0.1 to 8.33 g and 0.11 to 3.75 g in the well-watered and water-limited treatments, respectively. Cumulative transpiration ranged from 0 to 1470 ml in the well-watered and 0 to 379 ml in water-limited plants. There was a significant difference in dry biomass and transpiration rates between genotypes in both irrigation treatments and genotype x treatment effects (Fig. **1**; Table **1**), and across genotypes the water-limited treatment significantly reduced dry biomass and

transpiration by 54 and 72 %, respectively (Table **1**). The ratio of dry biomass relative to the amount of total transpiration (WUE_{plant}) was 58 % higher in the water-limited treatment and ranged across genotypes from 4.76 to 32.4 (g/L) in the well-watered treatment and 6.1 to 72.34 (g/L) in the water-limited treatment, respectively (Fig. **1**; Table **1**). Total transpiration was divided into daytime (T_{day}) and nighttime (T_{night}) components, where T_{day} and T_{night} ranged from 5 to 141 and 0 to 42 in the well-watered treatment, respectively and 2 to 69 and 0 to 30 in the water-limited treatment, respectively (Table **1**). Leaf N and C and C:N ratio were also measured and analyzed (Table **S1** and Table **S2**).

Broad-sense heritability, proportional variance and leaf carbon isotopic composition ($\delta^{13}C_{leaf}$)

In all traits, 15 - 72 % of the variance in the experiment was explained by the treatment effect (Table **2**). Additionally, in all traits, the variance ascribed to the genotype effect was relatively small but substantial given the large influence that the water limitation treatment had on these traits.

Broad-sense heritability (H^2) was relatively robust for all traits, including $\delta^{13}C_{leaf}$, in at least one treatment or when treatments were combined (Table **2**). For example, $\delta^{13}C_{leaf}$ was significantly heritable in the well-watered treatment (0.49) but not in the water-limited treatment (0.04), which was also the case with WUE_{plant} (0.19 and 0.02 in well-watered and water-limited, respectively). In all traits, the well-watered treatment had higher H^2 than the water-limited treatment. T_{night} had low H^2 values for both treatments (0.1 and 0.0 in well-watered and water-limited, respectively) that limited its strength in QTL analysis but H^2 was high when both treatments combined (0.43).

The $\delta^{13}C_{leaf}$ values ranged from -14.7 to -12.4 ‰ in the well-watered and -15.6 to -13.2 ‰ in the water-limited treatment, with significant differences across genotypes (Fig. **2**; Table **1**). The water-limited treatment significantly reduced $\delta^{13}C_{leaf}$ on average across genotypes by 0.82 ± 0.04 ‰ (Table **1**).

Correlation of traits with $\delta^{13}C_{leaf}$

Over the time course of the experiment, the correlations of $\delta^{13}C_{leaf}$ with dry biomass, transpiration, WUE_{plant}, T_{day}, and T_{night} were relatively constant over much of the experiment, and correlations were only lower in the beginning and end of the experiment (Fig. **2**). At the midpoint of the experiment (day 27), correlations with $\delta^{13}C_{leaf}$ were similar in magnitude to most days of the experiment (Fig. **S2**, **S3**, **S4**, **S5**, **S6**).

These correlations were stronger across treatments than within treatment, yet they were significant under the well-watered conditions (Fig. **2**). On day 27, the correlation coefficients of $\delta^{13}C_{leaf}$ with biomass, transpiration, T_{day}, and T_{night} were between 0.52 and 0.69 in magnitude across treatments and 0.25 to 0.42 for well-watered treatment (Fig. **3**). In the water-limited, correlations were low for all traits, with magnitudes ranging from -0.14 to 0.04 (Fig. **3**). On day 27, WUE_{plant} was negatively correlated with $\delta^{13}C_{leaf}$ with values of -0.60, -0.47, and -0.14 for both treatments combined, well-watered, and water-limited treatments, respectively.

QTL analysis and contributions of allele composition on traits

Three QTL (chr. 7@51 centimorgans (cM), chr. 7@99 cM and chr. 9@34 cM) associated with $\delta^{13}C_{leaf}$ were found in the well-watered treatment, but none were detected in the water-limited treatment (Table **3**). For simplicity, QTL were identified by their genomic position of the marker based on genetic linkage in centimorgans (cM) and was given the nomenclature of 'chromosome @ centimorgans'. No significant epistatic interaction between QTL was detected (Table **S3**). Two of these QTL (7@99, 9@34) co-localized with WUE_{plant}, dry biomass, transpiration, and T_{day} in both treatments on day 27. This pattern of co-localization of these two QTL is consistent over much of the experiment. QTL 7@51 was co-localized with cumulative transpiration and T_{night} in the well-watered treatment. Dry biomass was described in Feldman *et al.* (2018) as having this genetic architecture from days 17 through 33 (Table **3; S4**). Having an allele from parental accession A10 (*S. viridis*) at two of the three loci (7@51 and 7@99) increased $\delta^{13}C_{leaf}$ in the well-watered treatment, while an allele from parental line B100 (*S. italica*) increased $\delta^{13}C_{leaf}$ at 9@34 in both treatments (Fig. **S8**).

At each marker two alleles are possible, either the allele from the parental line A10 accession of *S. viridis* (A) or the allele from the other parent, B100 accession of *S. italica* (B). The RILs in the experiment were categorized in allele classes by combining the allele (represented by letters A or B) for the three QTL associated with $\delta^{13}C_{leaf}$ (in the following order: 7@51, 7@99, 9@34). The seven allele classes present in this population were AAA, AAB, ABB, BAA, BAB, BBA, and BBB, but allele class ABA was not present. For six of the seven allele classes, the SMA linear regression between dry biomass and transpiration was significant (Table **4**; Fig. **4a**). Furthermore, the regression of $\delta^{13}C_{leaf}$ against the slopes of dry biomass versus transpiration showed a strong negative relationship for both the well-watered ($\delta^{13}C_{leaf}$ = -0.146 slope – 12.27; R^2 = 0.88; P = 0.006)

and in the water-limited treatments ($\delta^{13}C_{leaf}$ = -0.0358 slope – 13.89; R^2 = 0.92, P = 0.0007; Fig. **4b**). Although this relationship was dampened in the water-limited treatment, it followed a similar trend (Fig. **4b**). Additionally, the order that the allele classes were positioned along the $\delta^{13}C_{leaf}$ versus slope regression is very similar between treatments. In the well-watered treatment, the QTL 7@99 (represented by the second letter in three-letter allele class names) appears to have the greatest influence on this relationship, where the A10 allele was associated with a reduced slope and enriched $\delta^{13}C_{leaf}$ (Fig. **4b**). Alternatively, in the water-limited treatment, the effect of QTL 7@99 on this relationship was reduced relative to the well-watered treatment. Additionally, in both treatements the mean dry biomass and transpiration for each of these allele classes had a strong significant positive relationship with $\delta^{13}C_{leaf}$ (Fig. **5a** and Fig. **5b**). Similar to the transpiration versus $\delta^{13}C_{leaf}$, T_{day} and T_{night} formed significant relationships with $\delta^{13}C_{leaf}$, but T_{night} formed a weaker relationship with $\delta^{13}C_{leaf}$ (Fig. **6a** and Fig. **6b**).

Discussion

Leaf carbon isotope composition ($\delta^{13}C_{leaf}$) has been theoretically related to TE_i (A_{net}/g_s) for both C_3 and C_4 species (Farquhar & Richards, 1984; Condon *et al.*, 1987; Henderson *et al.*, 1998; Condon *et al.*, 2002; Condon *et al.*, 2004). Despite the potential dampening effect that the CO_2-concentrating mechanism has on $\delta^{13}C_{leaf}$ variability in C_4 plants (von Caemmerer *et al.*, 2014), $\delta^{13}C_{leaf}$ in the *Setaria* RIL population presented here exhibited a significant genetic (range of 2.4 ‰) and environmental (mean difference of 0.82 ± 0.04 ‰ between treatments) effect. These results also show considerable genotype by treatment response, consistent with previous studies of well-watered and water-limited C_4 plants (Monneveux *et al.*, 2007; Cabrera-Bosquet, Llorenç *et al.*, 2009; Ellsworth *et al.*, 2017). In the well-watered treatment, the $\delta^{13}C_{leaf}$ had relatively strong correlations with WUE_{plant} and its component traits, biomass and transpiration. These correlations were consistent throughout much of the experiment and corroborate the theoretical relationship between $\delta^{13}C_{leaf}$ and WUE_{plant} through TE_i. However, in the water-limited plants the lack of significant correlations between $\delta^{13}C_{leaf}$ and other traits (e.g. WUE_{plant} , biomass, and transpiration) was likely due to restricted stomatal conductance (g_s) across most genotypes, minimizing individual differences in TE_i, similar to what was found in C_3 species (Lambrides *et al.*, 2004; Adiredjo *et al.*, 2014).

These data demonstrate a significant genetic and environmental influence on $\delta^{13}C_{leaf}$ in a C_4 species related to differences in WUE_{plant}. These relationships are further

supported by the fact that $\delta^{13}C_{leaf}$ shared a similar genetic architecture with WUE_{plant} and its component traits. For example, QTL (7@51, 7@99, 9@33) found for $\delta^{13}C_{leaf}$ are pleiotropic loci, co-localized with leaf composition traits and whole plant traits such as biomass production, transpiration, and WUE_{plant}. In the current study, WUE_{plant} was calculated differently from Feldman *et al.* (2018); however, the principal QTL for WUE_{plant} and its component traits remained similar between studies. The one notable difference was that the most significant QTL for WUE_{plant} calculated with transpiration (T) instead of ET shifted to 7@99 and 9@33. This highlights the apparent importance of using T in linking $\delta^{13}C_{leaf}$ to WUE_{plant}. This rationale is supported by theories describing the relationship between WUE_{plant} and $\delta^{13}C_{leaf}$, suggesting that in this RIL population TE_i has a greater influence on WUE_{plant} than the other components ϕ_w, ϕ_c, and r described in Theory section.

An additional trait that might influence the relationship between $\delta^{13}C_{leaf}$ and WUE_{plant} is bundle sheath leakiness (ϕ), where ϕ is defined as the ratio of bundle sheath CO_2 leak rate to the rate of PEP carboxylase. Changes in ϕ influence the relationship between $\Delta^{13}C_{leaf}$ and CO_2 availability (C_i/C_a) such that differences in $\delta^{13}C_{leaf}$ can result from variation in ϕ instead of TE_i. However, in this experiment it is unlikely that ϕ is the primary driver of $\delta^{13}C_{leaf}$. First, ϕ would have to be heritable to explain the genotypic effect in $\delta^{13}C_{leaf}$. Although this is possible there are no studies, that we are aware of, showing ϕ as heritable and under genetic control. Second, the consistent depletion in $\delta^{13}C_{leaf}$ in response to water limitation could occur if ϕ increased across all genotypes in the water-limited treatment. However, several studies have failed to find significant differences in ϕ under various environmental growth conditions including light gradients, salinity, and water limitation across species (Ubierna *et al.*, 2011; Bellasio, Chandra & Griffiths, Howard, 2014a; Bellasio, Chandra & Griffiths, Howard, 2014b; Bellasio, C. & Griffiths, H., 2014; Sharwood *et al.*, 2014; Sonawane *et al.*, 2017; Sonawane *et al.*, 2018; Sonawane and Cousins unpublished results). Third, ϕ-driven variation in $\delta^{13}C_{leaf}$ cannot explain the strong negative correlation between $\delta^{13}C_{leaf}$ and WUE_{plant} because increasing ϕ decreases the efficiency of the carbon-concentrating mechanism through overcycling (von Caemmerer *et al.*, 2014). This would decrease the photosynthetic efficiency, which, in turn, decreases TE_i and WUE_{plant}. Finally, the similar genetic architecture between $\delta^{13}C_{leaf}$ and WUE_{plant}, biomass and transpiration would not be expected if the variation in $\delta^{13}C_{leaf}$ was driven primarily by ϕ but rather TE_i. Therefore, variation in ϕ across individual plants could certainly contribute to $\delta^{13}C_{leaf}$,

potentially reducing the strength of the relationship between $\delta^{13}C_{leaf}$ and WUE_{plant}. Nonetheless, in this experiment there was a strong relationship between $\delta^{13}C_{leaf}$ and WUE_{plant} and its component traits.

Theoretical and empirical experiments indicate that $\delta^{13}C_{leaf}$ and TE_i should be negatively correlated (Farquhar, 1983; Henderson *et al.*, 1998; von Caemmerer *et al.*, 2014; Ellsworth *et al.*, 2017). Therefore, if TE_i is a strong component of WUE_{plant}, then there should also be a negative relationship between $\delta^{13}C_{leaf}$ and WUE_{plant}, as seen in the data presented here. In this RIL population there was a stronger relationship of $\delta^{13}C_{leaf}$ and WUE_{plant} across allele classes based on the three QTL for $\delta^{13}C_{leaf}$. The strong negative relationship between $\delta^{13}C_{leaf}$ and WUE_{plant} across these allele classes further supports the link of TE_i between $\delta^{13}C_{leaf}$ and WUE_{plant}. Across these allele classes, the relationship of $\delta^{13}C_{leaf}$ and WUE_{plant} is also seen in the water-limited treatment even though there were no QTL detected for $\delta^{13}C_{leaf}$ under this treatment. This is likely due to the dampened response of $\delta^{13}C_{leaf}$ to water-limited conditions as seen with previous studies (Avramova *et al.*, 2018). However, given that the water limitation did not remove the underlying relationship between TE_i and WUE_{plant}, the inability to detect QTL is likely due to the reduced variation in $\delta^{13}C_{leaf}$, which reduced the magnitude of the genotypic response and decreased the signal to noise ratio. Nonetheless, the basic relationship between $\delta^{13}C_{leaf}$ and WUE_{plant} remained in the water-limited treatment, as did the relative order of the allele classes. For example, under both well-watered and water-limited conditions the allele classes AAB and BAB had the lowest WUE_{plant} and most enriched $\delta^{13}C_{leaf}$. Whereas allele classes AAA and BAA were in the middle in both traits, and allele classes BBB and BBA had the highest WUE_{plant} and most depleted $\delta^{13}C_{leaf}$ under both treatments. This trend indicates a strong allelic effect on relationship between $\delta^{13}C_{leaf}$, TE_i, and WUE_{plant} that may allow $\delta^{13}C_{leaf}$ to be used as a proxy for TE_i, WUE_{plant} in well-watered and water-limited conditions.

Conclusion

WUE_{plant} is driven by a balance between carbon assimilation and water lost via stomates (TE_i) and other whole plant processes such as ϕ_c, ϕ_w, and r (when only aboveground biomass is measured). Hence, the relationship between $\delta^{13}C_{leaf}$ and WUE_{plant} is only apparent if TE_i has a strong influence on WUE_{plant}. In this C_4 grass RIL population, $\delta^{13}C_{leaf}$ showed a significant and consistent response to water limitation, significant genotypic variation, and significant heritability. Additionally, $\delta^{13}C_{leaf}$

correlated with transpiration, biomass, and WUE_{plant}, suggesting a physiological relationship among these traits. This is further supported by the fact that there were even stronger negative correlations between $\delta^{13}C_{leaf}$ and WUE_{plant} within the allele classes defined by QTL of $\delta^{13}C_{leaf}$. This suggests that differences in TE_i is driving the differences in both WUE_{plant} and $\delta^{13}C_{leaf}$. This relationship between $\delta^{13}C_{leaf}$ and WUE_{plant} across allele classes emphasizes the intrinsic role of TE_i in this relationship and implies that $\delta^{13}C_{leaf}$ can detect variation in WUE_{plant} when TE_i is a major driver of WUE_{plant}. The outcome of this research demonstrates that $\delta^{13}C_{leaf}$ has the potential to screen for TE_i in a marker-assisted C_4 plant breeding program. However, additional work is needed to better understand the genetic controls of $\delta^{13}C_{leaf}$, TE_i and WUE_{plant}. Furthermore, research is needed to explore the use of $\delta^{13}C_{leaf}$ in other C_4 species and under field settings to better understand the complex interaction of traits and causal genes that influence WUE_{plant}, TE_i, and $\delta^{13}C_{leaf}$.

Acknowledgements

This project was funded by U.S. Department of Energy (award number DE-SC0008769) to ABC and IB. ABC is supported in part by Meyer Distinguished Professorship. IB was supported by the US Department of Agriculture—Agricultural Research Service.

Author contributions

M.F. and I.B. performed the experiment; P.E and M.F. analyzed the results; P.E. wrote the manuscript; M.F., A.C., and I.B. contributed to the development and writing of the manuscript.

Appendix I Glossary of terms

Term	Definition
$\Delta^{13}C$	Photosynthetic carbon discrimination ($\delta^{13}C_{ambient}$ - $\delta^{13}C_{leaf}$)
$\delta^{13}C_{leaf}$	Leaf carbon isotopic composition (‰)
$\delta^{13}C_{ambient}$	Isotopic composition of ambient CO_2 (‰)
WUE_{ag}	Agricultural water use efficiency (crop yield/water applied to crop)
WUE_{plant}	Ratio of biomass accumulated per water transpired
TE_i	Intrinsic transpiration efficiency (A_{net}/g_s)
HI	Harvestable index
C_i/C_a	Intercellular to ambient CO_2 concentration
g_s	Stomatal conductance
A_{net}	Net photosynthetic rate
T	Transpiration rate
ET	Evapotranspiration
V	Evaporative demand; ($e_i - e_a$)
e_i - e_a	Water vapor molar difference between intercellular and ambient air at leaf temperature
ϕ_w	Proportion of water used by plant that is unproductive water loss (*e.g.* nighttime and cuticular transpiration)
ϕ_c	Proportion of fixed carbon lost through respiration
R	Proportion of biomass
A	Fractionation during diffusion of CO_2 in air through stomata (4.4 ‰)
T_{day}	Daytime transpiration (ml)
T_{night}	Nighttime transpiration (ml)
b_3	Fractionation by Rubisco (30 ‰)
b_4	Fractionation of PEP carboxylation and isotopic equilibrium during dissolution and hydration of CO_2 (–5.2 ‰ at a leaf temperature of 30 °C)
S	Fractionation during the CO_2 leakage from the bundle sheath cells (1.8 ‰)
Φ	Leakiness of CO_2 from the bundle sheath
H^2	Broad sense heritability

Table 1 Analysis of variance of traits.

Trait	Treatment block						Treatment		Genotype		Treatment x Genotype	
	Well-watered			Water-limited								
	Mean ± SE	Min	Max	Mean ± SE	Min	Max	$F_{ddf,ndf}$	*P*	$F_{ddf,ndf}$	*P*	$F_{ddf,ndf}$	*P*
Dry biomass (g)	4.91 ± 0.07	0.10	8.83	2.21 ± 0.02	0.11	3.75	$4968_{1,742}$	<0.001	$15.70_{188,742}$	<0.001	$5.71_{182,742}$	<0.001
Transpiration (ml)	565.3 ± 11.9	0.10	1470	159.5 ± 3.0	0.0	379.0	$2779_{1,764}$	<0.001	$7.468_{189,764}$	<0.001	$3.739_{183,764}$	<0.001
T_{day} (ml)	74.8 ± 1.0	5.0	141.0	31.9 ± 0.5	2.0	69.0	$2692_{1,764}$	<0.001	$5.398_{189,764}$	<0.001	$1.745_{183,764}$	<0.001
T_{night} (ml)	13.3 ± 0.3	0	42.0	6.8 ± 0.2	0	30.0	$290.8_{1,760}$	<0.001	$1.632_{189,760}$	<0.001	$0.393_{183,760}$	1.00
WUE_{plant} (g/L)	9.60 ± 0.14	4.76	32.40	15.14 ± 0.25	6.06	72.34	$515.8_{1,744}$	<0.001	$6.613_{188,744}$	<0.001	$1.063_{182,744}$	0.29
$\delta^{13}C_{leaf}$ (‰)	-13.50 ± 0.50	-14.86	-12.24	-14.33 ± 0.55	-15.99	-12.74	$569_{1,351}$	<0.001	$2.054_{184,351}$	<0.001	$1.003_{175,351}$	0.49

Means ± SD of fresh biomass, transpiration, WUE_{plant} were determined on day 27. $\delta^{13}C_{leaf}$ was collected at the end of the experiment on day 34. T_{day} and T_{night} are daily values for day 27, which was the first day that total transpiration could be separated into nighttime and daytime components.

Table 2 Proportional variance and broad-sense heritability (H^2) of traits on day 27 after sowing. $\delta^{13}C_{leaf}$ was collected at the end of the experiment. Transpiration is cumulative transpiration throughout the experiment, while T_{day} and T_{night} are daily volumes on day 27.

Trait	**Proportional variance**				**H^2**	
	Genotype	**Treatment**	**G x Treatment**	**Both treatments**	**Well-watered treatment**	**Water-limited treatment**
Dry biomass	0.14	0.67	0.11	0.65	0.78	0.68
Transpiration	0.11	0.65	0.11	0.57	0.62	0.39
T_{night}	0.09	0.72	0.04	0.43	0.10	0.00
T_{day}	0.08	0.34	0.00	0.67	0.51	0.21
WUE_{plant}	0.04	0.15	0.00	0.20	0.19	0.02
$\delta^{13}C_{leaf}$	0.09	0.55	0.01	0.45	0.49	0.04

Table 3. QTL found across all traits in both treatments that are co-localized in two or more traits. Colored cell represents at least one significant QTL found in the experiment.

Trait	Treatment	Genomic position of QTL											
		2@92	2@113	3@49	4@50	5@79	5@104	6@59	6@75	7@33	7@51	7@99	9@34
Dry biomass	well-watered	16.6	11.0	5.4		-9.4	-11.2	4.7	5.6	-4.5	-6.9	-9.4	9.2
	water-limited	11.4			11.7	-8.0	-8.3				-7.3	-6.8	18.3
Cumulative transpiration	well-watered	13.3		5.7			-8.7	4.2		-4.7	-5.9	-10.0	16.1
	water-limited	8.7			8.6		-7.0					-11.2	22.5
T_{night}	well-watered								5.6		-10.5		10.9
	water-limited												9.7
T_{day}	well-watered	10.7	8.8			-6.5	-5.0		4.4		-6.9	-9.0	15.9
	water-limited				5.7		-9.8	4.6				-6.2	20.7
$\delta^{13}C$	well-watered										-6.5	-8.2	14.5
	water-limited												
WUE_{plant}	well-watered					-8.8		8.2		5.7		15.1	-17.1
	water-limited					-10.5						8.6	-16.1

Filled cells represent QTL, and the number in the cell is the proportion of additive variance explained (%) by the QTL, which can have a positive or negative effect on the trait. All QTL found in the experiment are included in Table **S3**.

Table 4 $\delta^{13}C_{leaf}$ and the regression slope of the relationship between biomass and transpiration at the allele class level.

	Well-watered treatment					Water-limited treatment				
Allele class	**Slope**	**R^2**	***P***	**n**	**$\delta^{13}C_{leaf}$**	**Slope**	**R^2**	***P***	**n**	**$\delta^{13}C_{leaf}$**
AAA	7.02 ± 0.63	0.88	< 0.0001	26	-13.7 ± 0.08	13.01 ± 1.55	0.77	< 0.0001	26	-14.36 ± 0.07
AAB	7.11 ± 0.46	0.78	< 0.0001	64	-13.15 ± 0.04	11.08 ± 0.87	0.62	< 0.0001	64	-14.28 ± 0.05
ABA	Not present in RIL population									
ABB	7.71 ± 3.04	0.53	0.16	7	-13.8 ± 0.07	11.79 ± 1.63	0.93	0.008	7	-14.24 ± 0.16
BBB	12.09 ± 1.33	0.90	< 0.0001	13	-13.91 ± 0.07	14.00 ± 2.68	0. 74	0.003	13	-14.42 ± .13
BBA	11.71 ± 2.44	0.78	0.008	10	-14.0 ± 0.09	20.70 ± 3.24	0.90	0.004	10	-14.60 ± 0.10
BAB	7.14 ± 0.30	0.90	< 0.0001	68	-13.44 ± 0.04	10.97 ± 0.73	0.74	< 0.0001	68	-14.23 ± 0.05
BAA	9.50 ± 0.85	0.84	< 0.0001	28	-13.79 ± 0.09	45.56 ± 7.96	0.46	0.0005	28	-14.43 ± 0.08

The allele class 'ABA' was not present in this RIL population. These slopes ± SEM are from the relationship found in figure **4a** and are also plotted against $\delta^{13}C_{leaf}$ ± SEM in figure **4b**.

Figure captions

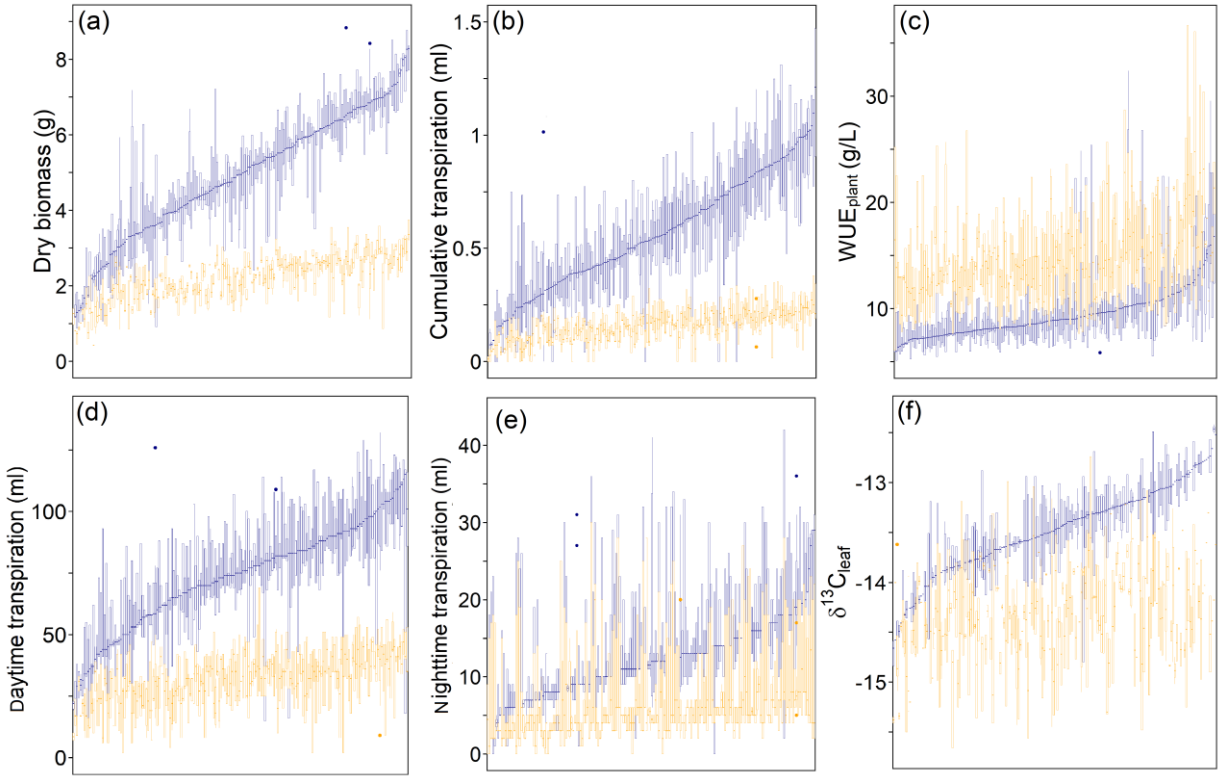

		Correlation (r) with $\delta^{13}C_{leaf}$			
Treatment	Dry biomass	Transpiration	WUE_{plant}	T_{day}	T_{night}
Well-watered	0.31	0.40	-0.47	0.42	0.25
Water-limited	-0.02	0.01	-0.14	0.04	-0.08
Both treatments	0.62	0.66	-0.60	0.69	0.52

Fig. 1 Ordered boxplots of dry biomass (A), transpiration (B), WUE_{plant} (C), T_{day} (D), T_{night} (E), and $\delta^{13}C_{leaf}$ (F). All traits were measured on day 27 at peak growth, except $\delta^{13}C_{leaf}$, which was measured on leaves collected at the end of the experiment on day 34. Treatment effect was significant for all traits. The table below shows the correlation coefficients of each trait from day 27 with $\delta^{13}C_{leaf}$.

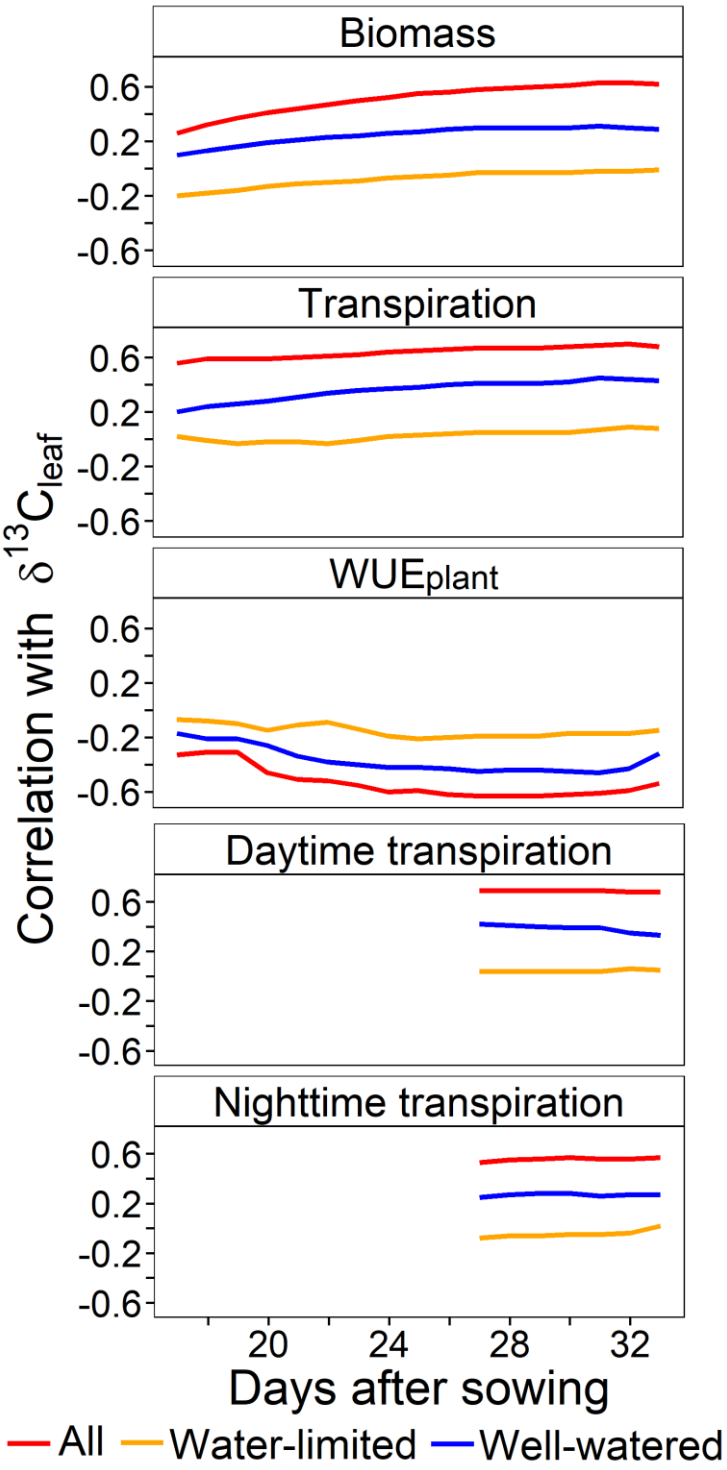

Fig. 2 Correlation (r) of dry biomass, transpiration, WUE_{plant}, T_{day}, and T_{night} with $\delta^{13}C_{leaf}$ through the course of the experiment. T_{day} and T_{night} were only available from day 27 to 33 because the daily irrigation schedule shifted to water when the lights turned on in the morning and when the lights turned off at night.

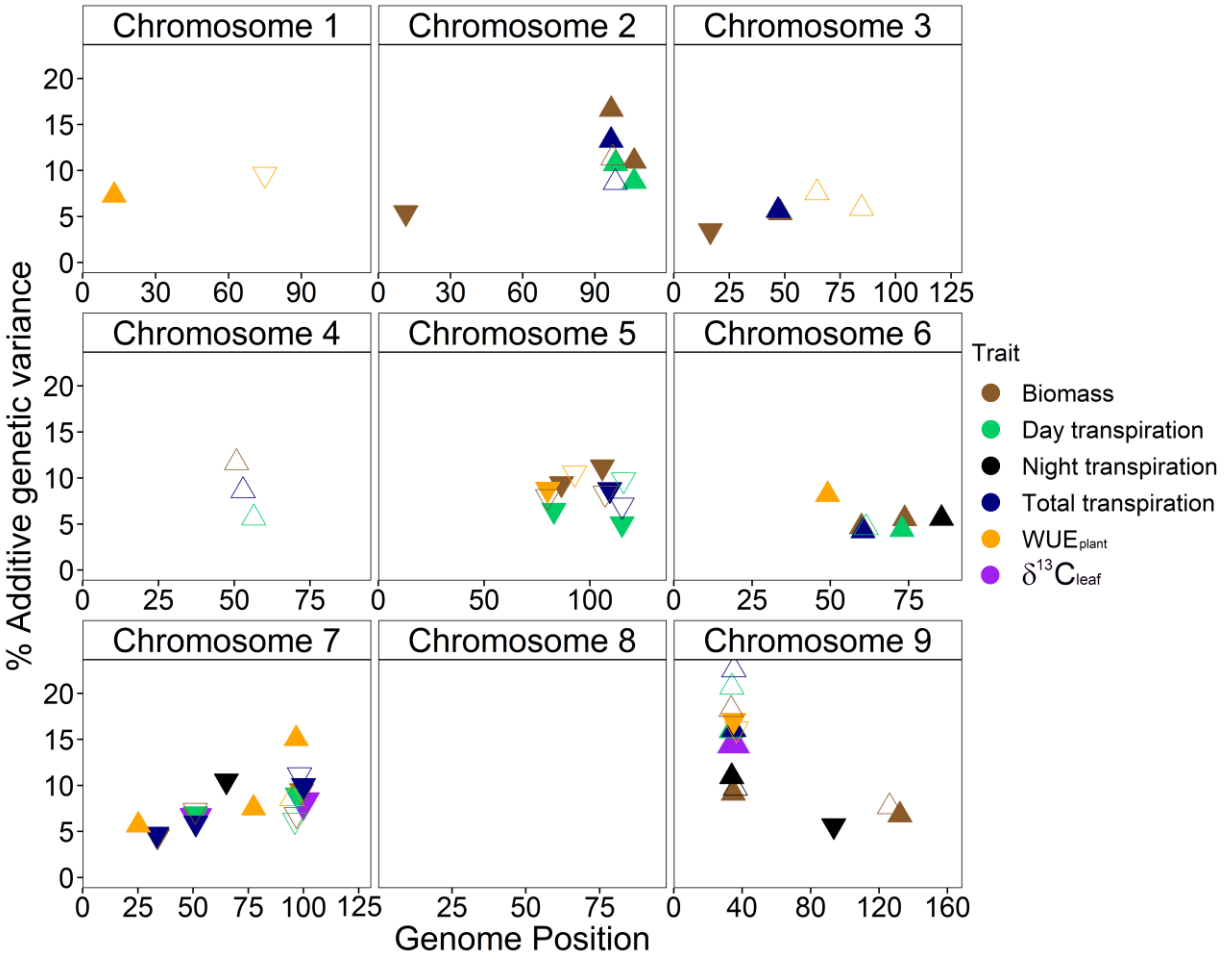

Fig. 3 Percent additive genetic variance of QTL of whole plant traits and $\delta^{13}C_{leaf}$, which was measured on leaves collected at the end of the experiment. Up-pointing and down-pointing triangles represent positive and negative mean proportional additive genetic variance, respectively. Filled and open triangles represent QTL from the well-watered and water-limited treatments, respectively.

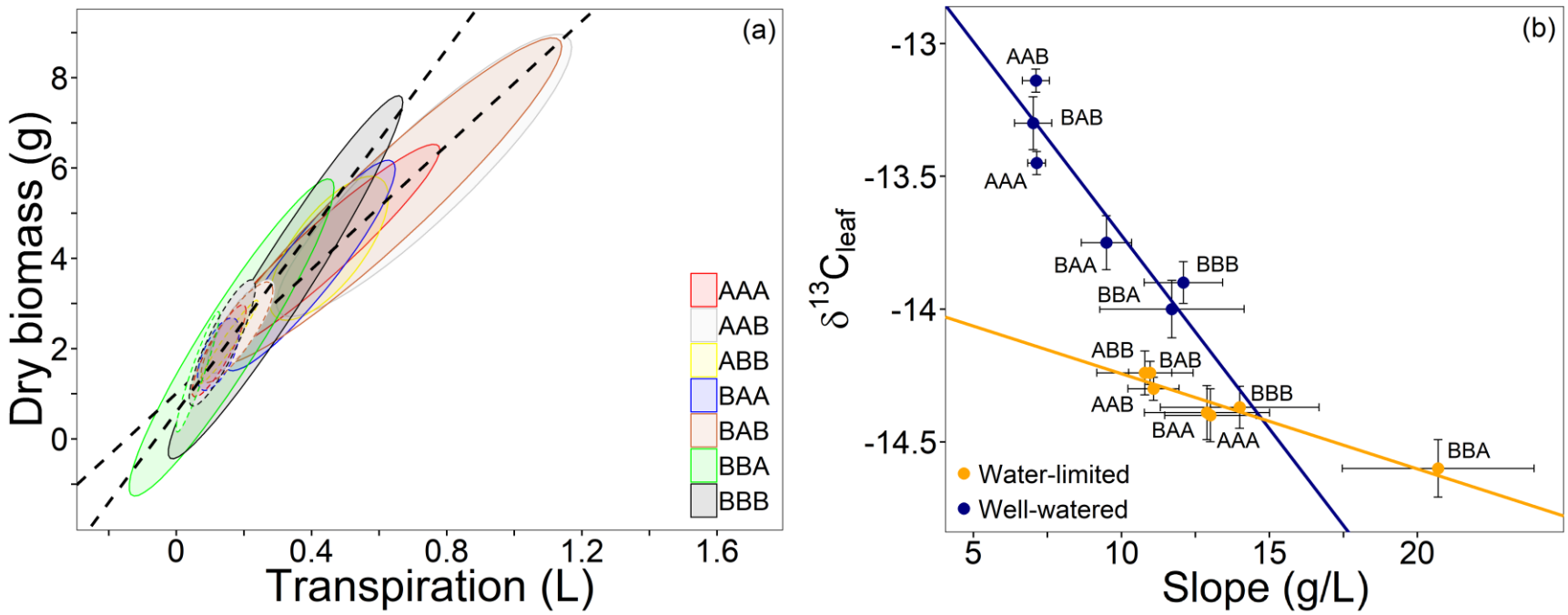

Fig. 4 The effect of allele class on dry biomass, transpiration, and $\delta^{13}C_{leaf}$. In panel (**a**), QTL 7@51, 7@99, and 9@34 were combined to produce seven alelle classes where the first letter represents the allele at QTL 7@51, the second letter represents the allele at QTL 7@99, and the third letter represents the allele at QTL 9@34. The letter 'A' represents the allele from the A10 parental accession (*Setaria viridis*), and 'B' represents the allele from the B100 parental accession (*Setaria italica*). Ellipses represent 95 % confidence intervals for the relationship of dry biomass and transpiration, and the slope of this relationship for each allele class was significant, except for allele class 'ABB' in the well-watered treatment ($P < 0.0001$). In panel (**b**), $\delta^{13}C_{leaf}$ ± SEM is regressed against the slope of relationship ± SEM in panel (**a**), excluding the non-significant slope for 'ABB'. The slope is the WUE_{plant} for an entire allele class. The regression for $\delta^{13}C_{leaf}$ versus slope was significant in the well-watered ($\delta^{13}C_{leaf} = -0.146$ slope – 12.27; $R^2 = 0.88$; $P = 0.006$) and in the water-limited treatments ($\delta^{13}C_{leaf} = -0.0358$ slope – 13.89; $R^2 = 0.92$, $P = 0.0007$).

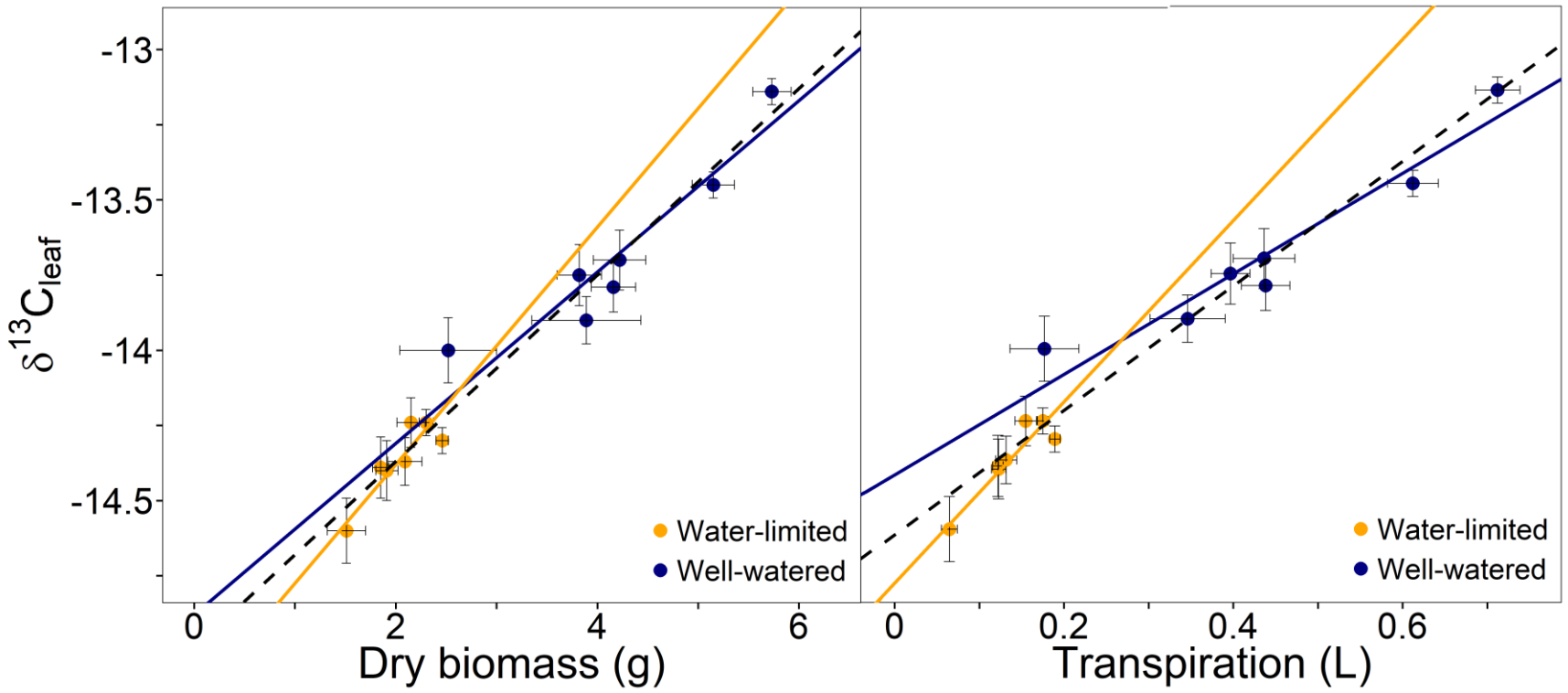

Fig. 5 The effect of allele class on the relationship of dry biomass and cumulative transpiration with $\delta^{13}C_{leaf}$. Like in Fig. **4**, QTL 7@51, 7@99 and 9@34 were combined to produce seven alelle classes. In panel **a**, the mean $\delta^{13}C_{leaf}$ was regressed against dry biomass for each treatment and both combined ($\delta^{13}C_{leaf}$ = 0.285 dry biomass – 14.88; R^2 = 0.87; P = 0.002 for well-watered; $\delta^{13}C_{leaf}$ = 0.395 dry biomass – 15.17; R^2 = 0.78; P = 0.008 for water-limited; $\delta^{13}C_{leaf}$ = 0.310 dry biomass – 14.99; R^2 = 0.96; P < 0.0001 for both treatments combined). In panel **b**, $\delta^{13}C_{leaf}$ is regressed against cumulative transpiration for treatment and both treatments combined ($\delta^{13}C_{leaf}$ = 1.67 transpiration – 14.42; R^2 = 0.92; P = 0.0006 for well-watered; $\delta^{13}C_{leaf}$ = 3.016 transpiration – 14.78; R^2 = 0.85; P = 0.003 for water-limited; $\delta^{13}C_{leaf}$ = 2.07 transpiration – 14.62; R^2 = 0.95; P < 0.0001 for both treatments). Regression of both treatments combined is identified by black, dashed line.

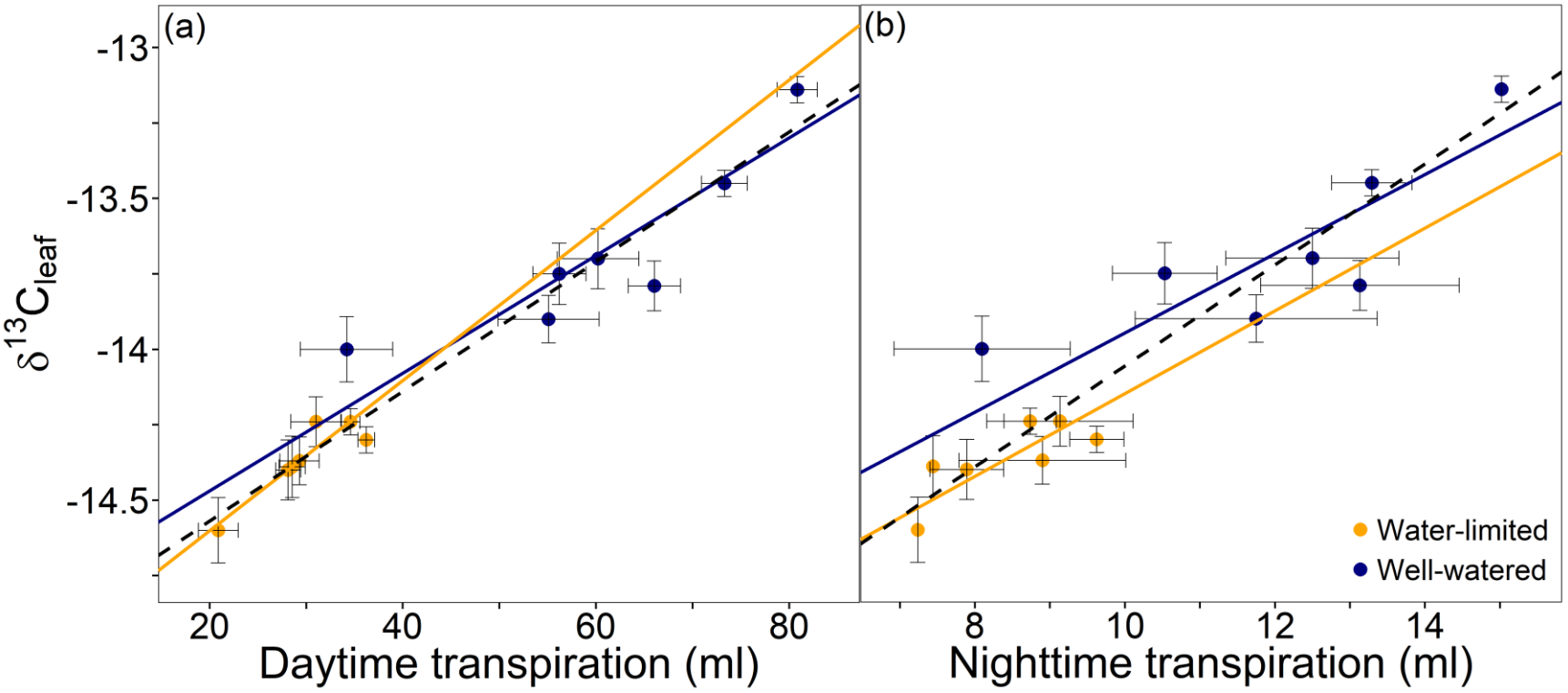

Fig. 6 The effect of allele class on the relationship of T_{day} and T_{night} with $\delta^{13}C_{leaf}$. Like in Fig. **4**, QTL 7@51, 7@99 and 9@34 were combined to produce seven alelle classes. In panel (**a**), the mean $\delta^{13}C_{leaf}$ was regressed against T_{day} and T_{night} for each treatment and both combined ($\delta^{13}C_{leaf}$ = 0.0195 T_{day} – 14.86; R^2 = 0.78; P = 0.008 for well-watered; $\delta^{13}C_{leaf}$ = 0.0249 T_{day} – 15.10; R^2 = 0.81; P = 0.006 for water-limited; $\delta^{13}C_{leaf}$ = 0.0215 T_{day} – 15.00; R^2 = 0.93; P < 0.0001). In panel (**b**), $\delta^{13}C_{leaf}$ is regressed against T_{night} for each treatment and both treatments combined ($\delta^{13}C_{leaf}$ = 0.131 T_{night} – 15.26; R^2 = 0.67; P = 0.02 for well-watered; $\delta^{13}C_{leaf}$ = 0.137 T_{night} – 15.52; R^2 = 0.60; P = 0.04 for water-limited; $\delta^{13}C_{leaf}$ = 0.167 T_{night} – 15.73; R^2 = 0.85; P < 0.0001 for both treatments). Regression of both treatments combined is identified by black, dashed line. These values of transpiration represent transpiration on day 27 only because day 27 was the first day that T_{day} and T_{night} could be separated.

References Cited

Adiredjo AL, Navaud O, Muños S, Langlade NB, Lamaze T, Grieu P. 2014. Genetic control of water use efficiency and leaf carbon isotope discrimination in sunflower (*Helianthus annuus* L.) subjected to two drought scenarios. *PLoS ONE* **9**(7): e101218-e101218.

Araus JL, Cabrera-Bosquet L, Serret MD, Bort J, Nieto-Taladriz MT. 2013. Comparative performance of $\delta^{13}C$, $\delta^{18}O$ and $\delta^{15}N$ for phenotyping durum wheat adaptation to a dryland environment. *Functional Plant Biology* **40**(6): 595-608.

Avramova V, Meziane A, Bauer E, Blankenagel S, Eggels S, Gresset S, Grill E, Niculaes C, Ouzunova M, Poppenberger B. 2018. Carbon isotope composition, water use efficiency, and drought sensitivity are controlled by a common genomic segment in maize. *Theoretical and Applied Genetics*: 1-11.

Bellasio C, Griffiths H. 2014. Acclimation of C_4 metabolism to low light in mature maize leaves could limit energetic losses during progressive shading in a crop canopy. *Journal of Experimental Botany* **65**(13): 3725-3736.

Bellasio C, Griffiths H. 2014a. Acclimation to low light by C_4 maize: implications for bundle sheath leakiness. *Plant, Cell & Environment* **37**(5): 1046-1058.

Bellasio C, Griffiths H. 2014b. The operation of two decarboxylases, transamination, and partitioning of C_4 metabolic processes between mesophyll and bundle sheath cells allows light capture to be balanced for the maize C_4 pathway. *Plant Physiology* **164**(1): 466-480.

Bierhuizen J, Slatyer R. 1965. Effect of atmospheric concentration of water vapour and CO_2 in determining transpiration-photosynthesis relationships of cotton leaves. *Agricultural Meteorology* **2**(4): 259-270.

Brendel O, Le Thiec D, Scotti-Saintagne C, Bodénès C, Kremer A, Guehl J-M. 2008. Quantitative trait loci controlling water use efficiency and related traits in *Quercus robur* L. *Tree Genetics & Genomes* **4**(2): 263-278.

Brenna JT, Corso TN, Tobias HJ, Caimi RJ. 1997. High-precision continuous-flow isotope ratio mass spectrometry. *Mass Spectrometry Reviews* **16**(5): 227-258.

Cabrera-Bosquet L, Molero G, Nogués S, Araus JL. 2009. Water and nitrogen conditions affect the relationships of $\Delta^{13}C$ and $\Delta^{18}O$ to gas exchange and growth in durum wheat. *Journal of Experimental Botany* **60**(6): 1633-1644.

Cabrera-Bosquet L, Sánchez C, Araus JL. 2009. How yield relates to ash content, $\Delta^{13}C$ and $\Delta^{18}O$ in maize grown under different water regimes. *Annals of Botany* **104**(6): 1207-1216.

Cabrera-Bosquet L, Albrizio R, Nogués S, Araus JL. 2011. Dual $\Delta^{13}C/\delta^{18}O$ response to water and nitrogen availability and its relationship with yield in field-grown durum wheat. *Plant, Cell & Environment* **34**(3): 418-433.

Cabrera-Bosquet L, Crossa J, von Zitzewitz J, Serret MD, Luis Araus J. 2012. High-throughput phenotyping and genomic selection: The frontiers of crop breeding converge. *Journal of Integrative Plant Biology* **54**(5): 312-320.

Cabrera-Bosquet L, Sánchez C, Araus JL. 2009. Oxygen isotope enrichment ($\Delta^{18}O$) reflects yield potential and drought resistance in maize. *Plant, Cell & Environment* **32**(11): 1487-1499.

Cerasoli S, Maillard P, Scartazza A, Brugnoli E, Chaves MM, Pereira JS. 2004. Carbon and nitrogen winter storage and remobilisation during seasonal flush growth in two-year-old cork oak (*Quercus suber* L.) saplings. *Annals of Forest Science* **61**: 721-729.

Chambers JM, Hastie TJ. 1992. *Statistical models in S*: Wadsworth & Brooks/Cole Advanced Books & Software Pacific Grove, CA.

Chaves MM, Santos TP, Souza CRd, Ortuño M, Rodrigues M, Lopes C, Maroco J, Pereira JS. 2007. Deficit irrigation in grapevine improves water-use efficiency while controlling vigour and production quality. *Annals of Applied Biology* **150**(2): 237-252.

Condon AG, Richards RA, Farquhar GD. 1987. Carbon isotope discrimination is positively correlated with grain yield and dry matter production in field-grown wheat. *Crop Science* **27**(5): 996-1001.

Condon AG, Richards RA, Rebetzke GJ, Farquhar GD. 2002. Improving intrinsic water-use efficiency and crop yield. *Crop Science* **42**(1): 122-131.

Condon AG, Richards RA, Rebetzke GJ, Farquhar GD. 2004. Breeding for high water-use efficiency. *Journal of Experimental Botany* **55**(407): 2447-2460.

Coupel-Ledru A, Lebon E, Christophe A, Gallo A, Gago P, Pantin F, Doligez A, Simonneau T. 2016. Reduced nighttime transpiration is a relevant breeding target for high water-use efficiency in grapevine. *Proceedings of the National Academy of Sciences of the United States of America* **113**(32): 8963-8968.

Deng X-P, Shan L, Zhang H, Turner NC. 2006. Improving agricultural water use efficiency in arid and semiarid areas of China. *Agricultural Water Management* **80**(1): 23-40.

Des Marais DL, Razzaque S, Hernandez KM, Garvin DF, Juenger TE. 2016. Quantitative trait loci associated with natural diversity in water-use efficiency and response to soil drying in *Brachypodium distachyon*. *Plant Science* **251**: 2-11.

Devos KM, Wang Z, Beales J, Sasaki T, Gale M. 1998. Comparative genetic maps of foxtail millet (*Setaria italica*) and rice (*Oryza sativa*). *Theoretical and Applied Genetics* **96**(1): 63-68.

Dhanapal AP, Ray JD, Singh SK, Hoyos-Villegas V, Smith JR, Purcell LC, King CA, Cregan PB, Song Q, Fritschi FB. 2015. Genome-wide association study (GWAS) of carbon isotope ratio ($\delta^{13}C$) in diverse soybean [*Glycine max* (L.) Merr.] genotypes. *Theoretical and Applied Genetics* **128**(1): 73-91.

Doust AN, Kellogg EA, Devos KM, Bennetzen JL. 2009. Foxtail millet: a sequence-driven grass model system. *Plant Physiology* **149**(1): 137-141.

Easlon HM, Nemali KS, Richards JH, Hanson DT, Juenger TE, McKay JK. 2014. The physiological basis for genetic variation in water use efficiency and carbon isotope composition in *Arabidopsis thaliana*. *Photosynthesis Research* **119**(1-2): 119-129.

Elazab A, Molero G, Serret MD, Araus JL. 2012. Root traits and $\delta^{13}C$ and $\delta^{18}O$ of durum wheat under different water regimes. *Functional Plant Biology* **39**(5): 379-393.

Ellsworth PZ, Ellsworth PV, Cousins A. 2017. Leaf oxygen and carbon isotopic signatures reflect drought resistance and water use efficiency in the C_4 grasses *Setaria viridis* and *Setaria italica*. *Journal of Experimental Botany* **68**(13): 3513-3528.

Fahlgren N, Feldman M, Gehan MA, Wilson MS, Shyu C, Bryant DW, Hill ST, McEntee CJ, Warnasooriya SN, Kumar I. 2015. A versatile phenotyping system and analytics platform reveals diverse temporal responses to water availability in *Setaria*. *Molecular Plant* **8**(10): 1520-1535.

Farquhar GD. 1983. On the nature of carbon isotope discrimination in C_4 species. *Functional Plant Biology* **10**(2): 205-226.

Farquhar GD, Ehleringer JR, Hubick KT. 1989. Carbon isotope discrimination and photosynthesis. *Annual Review of Plant Biology* **40**(1): 503-537.

Farquhar GD, Hubick KT, Condon AG, Richards RA 1989. Carbon isotope fractionation and plant water-use efficiency. *Stable isotopes in ecological research*: Springer, 21-40.

Farquhar GD, Richards RA. 1984. Isotopic composition of plant carbon correlates with water-use efficiency of wheat genotypes. *Australian Journal of Plant Physiology* **11**(6): 539-552.

Feldman MJ, Ellsworth PZ, Fahlgren N, Gehan MA, Cousins AB, Baxter I. 2018. Trait components of whole plant water use efficiency are defined by unique, environmentally responsive genetic signatures in the model C_4 grass *Setaria*. *Plant Physiology*.

Feldman MJ, Paul RE, Banan D, Barrett JF, Sebastian J, Yee M-C, Jiang H, Lipka AE, Brutnell TP, Dinneny JR, et al. 2017. Time dependent genetic analysis links field and controlled environment phenotypes in the model C_4 grass *Setaria*. *PLoS Genetics* **13**(6): e1006841.

Flexas J, GalméS J, Gallé A, Gullás J, Pou A, Ribas-Carbo M, TomáS M, Medrano H. 2010. Improving water use efficiency in grapevines: potential physiological targets for biotechnological improvement. *Australian Journal of Grape and Wine Research* **16**: 106-121.

Ghannoum O. 2016. How can we breed for more water use-efficient sugarcane? *Journal of Experimental Botany* **67**(3): 557-559.

Gibberd MR, Walker RR, Blackmore DH, Condon AG. 2001. Transpiration efficiency and carbon-isotope discrimination of grapevines grown under well-watered conditions in either glasshouse or vineyard. *Australian Journal of Grape and Wine Research* **7**(3): 110-117.

Gresset S, Westermeier P, Rademacher S, Ouzunova M, Presterl T, Westhoff P, Schon CC. 2014. Stable carbon isotope discrimination is under genetic control in the C_4 species maize with several genomic regions influencing trait expression. *Plant Physiology* **164**(1): 131-143.

Henderson S, Von Caemmerer S, Farquhar GD, Wade L, Hammer G. 1998. Correlation between carbon isotope discrimination and transpiration efficiency in lines of the C_4 species *Sorghum bicolor* in the glasshouse and the field. *Functional Plant Biology* **25**(1): 111-123.

Henderson SA, Caemmerer SV, Farquhar GD. 1992. Short-term measurements of carbon isotope discrimination in several C_4 species. *Functional Plant Biology* **19**(3): 263-285.

Juenger TE, McKay JK, Hausmann N, Keurentjes JJB, Sen S, Stowe KA, Dawson TE, Simms EL, Richards JH. 2005. Identification and characterization of QTL underlying whole-plant physiology in *Arabidopsis thaliana*: $\delta^{13}C$, stomatal conductance and transpiration efficiency. *Plant, Cell & Environment* **28**(6): 697-708.

Kromdijk J, Ubierna N, Cousins AB, Griffiths H. 2014. Bundle-sheath leakiness in C_4 photosynthesis: a careful balancing act between CO_2 concentration and assimilation. *Journal of Experimental Botany* **65**(13): 3443-3457.

Kubásek J, Šetlík J, Dwyer S, Šantrůček J. 2007. Light and growth temperature alter carbon isotope discrimination and estimated bundle sheath leakiness in C_4 grasses and dicots. *Photosynthesis Research* **91**(1): 47-58.

Kwak I-Y, Moore CR, Spalding EP, Broman KW. 2016. Mapping quantitative trait loci underlying function-valued traits using functional principal component analysis and multi-trait mapping. *G3: Genes| Genomes| Genetics* **6**(1): 79-86.

Lambrides C, Chapman S, Shorter R. 2004. Genetic variation for carbon isotope discrimination in sunflower. *Crop Science* **44**(5): 1642-1653.

Masle J, Gilmore SR, Farquhar GD. 2005. The ERECTA gene regulates plant transpiration efficiency in *Arabidopsis*. *Nature* **436**(7052): 866-870.

McKay JK, Richards JH, Nemali KS, Sen S, Mitchell-Olds T, Boles S, Stahl EA, Wayne T, Juenger TE. 2008. Genetics of drought adaptation in *Arabidopsis thaliana* II. QTL Analysis of a new mapping population, Kas-1× Tsu-1. *Evolution* **62**(12): 3014-3026.

Medrano H, Tomás M, Martorell S, Escalona J-M, Pou A, Fuentes S, Flexas J, Bota J. 2015a. Improving water use efficiency of vineyards in semi-arid regions. A review. *Agronomy for Sustainable Development* **35**(2): 499-517.

Medrano H, Tomás M, Martorell S, Flexas J, Hernández E, Rosselló J, Pou A, Escalona J-M, Bota J. 2015b. From leaf to whole-plant water use efficiency (WUE) in complex canopies: limitations of leaf WUE as a selection target. *The Crop Journal* **3**(3): 220-228.

Monneveux P, Sheshshayee MS, Akhter J, Ribaut J-M. 2007. Using carbon isotope discrimination to select maize (*Zea mays* L.) inbred lines and hybrids for drought tolerance. *Plant Science* **173**(4): 390-396.

Mook WG, Bommerson JC, Staverman WH. 1974. Carbon isotope fractionation between dissolved bicarbonate and gaseous carbon dioxide. *Earth and Planetary Science Letters* **22**(2): 169-176.

Morison JI, Baker NR, Mullineaux PM, Davies WJ. 2008. Improving water use in crop production. *Philosophical Transactions of the Royal Society of London B: Biological Sciences* **363**(1491): 639-658.

Passioura J. 1977. Grain yield, harvest index, and water use of wheat. *Journal of the Australian Institute of Agricultural Science* **43**: 117-120.

Pinto H, Powell JR, Sharwood RE, Tissue DT, Ghannoum O. 2015. Variations in nitrogen use efficiency reflect the biochemical subtype while variations in water use efficiency reflect the evolutionary lineage of C_4 grasses at inter-glacial CO_2. *Plant, Cell & Environment* **39**(3): 514-526.

Poni S, Bernizzoni F, Civardi S, Gatti M, Porro D, Camin F. 2009. Performance and water-use efficiency (single-leaf vs. whole-canopy) of well-watered and half-stressed split-root Lambrusco grapevines grown in Po Valley (Italy). *Agriculture, Ecosystems & Environment* **129**(1): 97-106.

Qi H, Coplen TB, Geilmann H, Brand WA, Böhlke JK. 2003. Two new organic reference materials for $\delta^{13}C$ and $\delta^{15}N$ measurements and a new value for the $\delta^{13}C$ of NBS 22 oil. *Rapid Communications in Mass Spectrometry* **17**(22): 2483-2487.

R_Core_Team 2013. R: A language and environment for statistical computing. Vienna, Austria: R Foundation for Statistical Computing.

Rebetzke GJ, Condon AG, Farquhar GD, Appels R, Richards RA. 2008. Quantitative trait loci for carbon isotope discrimination are repeatable across environments and wheat mapping populations. *Theoretical and Applied Genetics* **118**(1): 123-137.

Richards RA, Hunt JR, Kirkegaard JA, Passioura JB. 2014. Yield improvement and adaptation of wheat to water-limited environments in Australia—a case study. *Crop and Pasture Science* **65**(7): 676-689.

Sage RF. 2014. Stopping the leaks: new insights into C_4 photosynthesis at low light. *Plant, Cell & Environment* **37**(5): 1037-1041.

Santrock J, Studley SA, Hayes JM. 1985. Isotopic analyses based on the mass spectra of carbon dioxide. *Analytical Chemistry* **57**(7): 1444-1448.

Saranga Y, Jiang CX, Wright R, Yakir D, Paterson A. 2004. Genetic dissection of cotton physiological responses to arid conditions and their inter-relationships with productivity. *Plant, Cell & Environment* **27**(3): 263-277.

Seibt U, Rajabi A, Griffiths H, Berry JA. 2008. Carbon isotopes and water use efficiency: sense and sensitivity. *Oecologia* **155**(3): 441-454.

Sharwood RE, Sonawane BV, Ghannoum O. 2014. Photosynthetic flexibility in maize exposed to salinity and shade. *Journal of Experimental Botany* **65**(13): 3715-3724.

Sinclair TR, Tanner C, Bennett J. 1984. Water-use efficiency in crop production. *Bioscience* **34**(1): 36-40.

Sonawane BV, Sharwood RE, von Caemmerer S, Whitney SM, Ghannoum O. 2017. Short-term thermal photosynthetic responses of C_4 grasses are independent of the biochemical subtype. *Journal of Experimental Botany* **68**(20): 5583-5597.

Sonawane BV, Sharwood RE, Whitney S, Ghannoum O. 2018. Shade compromises the photosynthetic efficiency of NADP-ME less than that of PEP-CK and NAD-ME C_4 grasses. *Journal of Experimental Botany* **69**(12): 3053-3068.

Sun W, Ubierna N, Ma J-Y, Cousins AB. 2012. The influence of light quality on C_4 photosynthesis under steady-state conditions in *Zea mays* and *Miscanthus* × *giganteus*: changes in rates of photosynthesis but not the efficiency of the CO_2 concentrating mechanism. *Plant, Cell & Environment* **35**(5): 982-993.

Takai T, Fukuta Y, Sugimoto A, Shiraiwa T, Horie T. 2006. Mapping of QTLs controlling carbon isotope discrimination in the photosynthetic system using recombinant inbred lines derived from a cross between two different rice (*Oryza sativa* L.) cultivars. *Plant Production Science* **9**(3): 271-280.

Takai T, Ohsumi A, San-oh Y, Laza MRC, Kondo M, Yamamoto T, Yano M. 2009. Detection of a quantitative trait locus controlling carbon isotope discrimination and its contribution to stomatal conductance in japonica rice. *Theoretical and Applied Genetics* **118**(7): 1401-1410.

Tarara JM, Peña JEP, Keller M, Schreiner RP, Smithyman RP. 2011. Net carbon exchange in grapevine canopies responds rapidly to timing and extent of regulated deficit irrigation. *Functional Plant Biology* **38**(5): 386-400.

Terashima I, Hikosaka K. 1995. Comparative ecophysiology of leaf and canopy photosynthesis. *Plant, Cell & Environment* **18**(10): 1111-1128.

Teulat B, Merah O, Sirault X, Borries C, Waugh R, This D. 2002. QTLs for grain carbon isotope discrimination in field-grown barley. *TAG Theoretical and Applied Genetics* **106**(1): 118-126.

Thumma BR, Naidu BP, Chandra A, Cameron DF, Bahnisch LM, Liu C. 2001. Identification of causal relationships among traits related to drought resistance in *Stylosanthes scabra* using QTL analysis. *Journal of Experimental Botany* **52**(355): 203-214.

Tomás M, Medrano H, Escalona JM, Martorell S, Pou A, Ribas-Carbó M, Flexas J. 2014. Variability of water use efficiency in grapevines. *Environmental and Experimental Botany* **103**: 148-157.

Tomás M, Medrano H, Pou A, Escalona JM, Martorell S, Ribas-Carbó M, Flexas J. 2012. Water-use efficiency in grapevine cultivars grown under controlled conditions: effects of

water stress at the leaf and whole-plant level. *Australian Journal of Grape and Wine Research* **18**(2): 164-172.

Twohey III RJ, Roberts LM, Studer AJ. 2018. Leaf stable carbon isotope composition reflects transpiration efficiency in *Zea mays*. *The Plant Journal*.

Ubierna N, Sun W, Cousins AB. 2011. The efficiency of C_4 photosynthesis under low light conditions: assumptions and calculations with CO_2 isotope discrimination. *Journal of Experimental Botany* **62**(9): 3119-3134.

Vadez V, Kholova J, Medina S, Kakkera A, Anderberg H. 2014. Transpiration efficiency: new insights into an old story. *Journal of Experimental Botany* **65**(21): 6141-6153.

von Caemmerer S, Ghannoum O, Pengelly JJ, Cousins AB. 2014. Carbon isotope discrimination as a tool to explore C_4 photosynthesis. *Journal of Experimental Botany* **65**(13): 3459-3470.

Wang Z, Devos K, Liu C, Wang R, Gale M. 1998. Construction of RFLP-based maps of foxtail millet, *Setaria italica* (L.) P. Beauv. *Theoretical and Applied Genetics* **96**(1): 31-36.

Westgate M, Forcella F, Reicosky D, Somsen J. 1997. Rapid canopy closure for maize production in the northern US corn belt: radiation-use efficiency and grain yield. *Field Crops Research* **49**(2-3): 249-258.

Xu L-K, Hsiao TC. 2004. Predicted versus measured photosynthetic water-use efficiency of crop stands under dynamically changing field environments. *Journal of Experimental Botany* **55**(407): 2395-2411.

Xu X, Martin B, Comstock JP, Vision TJ, Tauer CG, Zhao B, Pausch RC, Knapp S. 2008. Fine mapping a QTL for carbon isotope composition in tomato. *Theoretical and Applied Genetics* **117**(2): 221-233.

Xu Y, This D, Pausch RC, Vonhof WM, Coburn JR, Comstock JP, McCouch SR. 2009. Leaf-level water use efficiency determined by carbon isotope discrimination in rice seedlings: genetic variation associated with population structure and QTL mapping. *Theoretical and Applied Genetics* **118**(6): 1065-1081.

Yousfi S, Serret MD, Márquez AJ, Voltas J, Araus JL. 2012. Combined use of $\delta^{13}C$, $\delta^{18}O$ and $\delta^{15}N$ tracks nitrogen metabolism and genotypic adaptation of durum wheat to salinity and water deficit. *New Phytologist* **194**(1): 230-244.